ChemComm

Z-Selective Dimerization of Terminal Alkynes by a (PNNP)Fe^{II} Complex

Journal:	*ChemComm*
Manuscript ID	CC-COM-01-2024-000469.R1
Article Type:	Communication

COMMUNICATION

Z-Selective Dimerization of Terminal Alkynes by a (PNNP)Fe^{II} Complex

Received 00th January 20xx,
Accepted 00th January 20xx

DOI: 10.1039/x0xx00000x

Jeremiah E. Stevens,[a] Justin D. Miller,[a] Matthew C. Fitzsimmons,[a] Curtis E. Moore,[a] and Christine M. Thomas*[a]

A tetradentate bis(amido)bis(phosphine) Fe^{II} complex, (PNNP)Fe, is shown to activate the terminal C–H bond of aryl alkynes across its Fe–N$_{amide}$ bonds. (PNNP)Fe is also shown to catalytically dimerize terminal aryl alkynes to produce 1,3-enynes with *Z:E* ratios as high as 96:4 with yields up to 95% with loadings as low as 1 mol% at 30 °C in 2 h. A plausible metal-ligand cooperative mechanism invoking a vinylidene intermediate is proposed.

Conjugated 1,3-enynes are useful synthons for the construction of more complex structures including natural products, substituted arenes and heterocycles, and organic materials.[1–6] While the most established method to form 1,3-enynes is Sonogashira coupling,[7,8] the dimerization of terminal alkynes is an attractive alternative (Fig. 1a), as the transformation is atom economical and applicable to the wide array of commercial terminal alkynes.[9] Challenges with controlling the chemo-, regio-, and stereoselectivity of alkyne dimerization have, until recently, limited the applications of this approach, though many precious metal-based homogeneous catalysts for alkyne dimerization have been investigated in detail.[9–11]

Due to the availability, cost efficiency, and low environmental impact of Fe salts, Fe-based homogeneous catalysts have emerged as an attractive target for alkyne dimerization.[12,13] In the first report of Fe-catalyzed alkyne dimerization, Dash and co-workers used 30 mol % $FeCl_3$, 30 mol % amine or phosphine ligand, and 300 mol % KO^{t}Bu at 145 °C for 2 h to yield enyne products with *E:Z* ratios up to 83:17.[14,15] Subsequent research efforts sought to develop Fe catalysts with better-defined mechanisms hoping to better control regio- and stereoselectivity. Initial efforts employed well-defined homogeneous Fe catalysts but required elevated temperatures (120-145 °C) and large quantities of MO^{t}Bu (M = K or Na) as an activator.[16,17] In contrast, Song and co-workers developed a series of cyclopentadienyl Fe complexes capable of radical-free 100% *gem*-selective alkyne dimerization at room temperature in under 1 hour with ≤ 5 mol % [Fe].[18–20] Milstein and Kirchner developed PNP pincer-ligated Fe complexes that effect highly *Z*-selective dimerization at room temperature without the need for additives (Fig. 1b).[21–23] Similarly, an N-heterocyclic carbene (NHC) Fe pincer complex developed by de Ruiter and co-workers was shown to dimerize alkynes at room temperature with *E:Z* ratios of 1:99 with a variety of terminal aryl alkynes.[24]

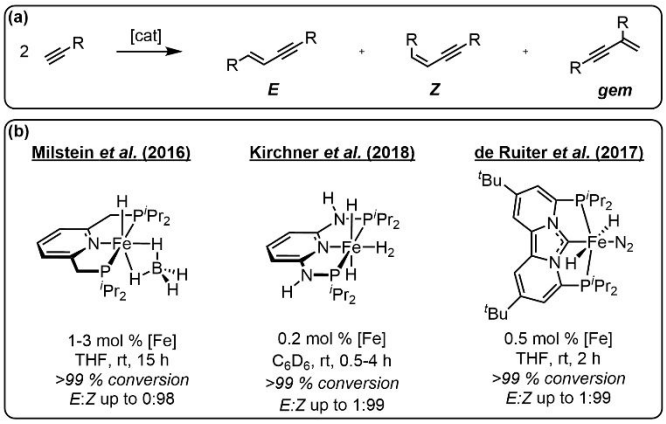

Fig. 1: (a) Possible 1,3-enynes resulting from the dimerization of terminal alkynes. (b) Selected examples of *Z*-selective homogeneous Fe-based (pre)catalysts for the dimerization of terminal alkynes

Our group has recently reported a square planar aryl-linked tetradentate bis(phosphine)bis(amido) Fe^{II} complex, (PNNP)Fe (**1**), and its activation of B–H and Si–H bonds across the Fe–N$_{amide}$ bonds.[25,26] Positing that similar activity would be observed with acidic C–H bonds, we were inspired to treat **1** with terminal alkynes (pK_a ≈ 25). Herein, we report an Fe bis(phenylacetylide) complex resulting from the addition of 2 equiv phenylacetylene to **1** and show that this metal-ligand

[a] *Department of Chemistry and Biochemistry, The Ohio State University, 100 W. 18th Ave., Columbus, OH 43210 USA.*
* Corresponding author. Email: thomasc@chemistry.ohio-state.edu
Electronic Supplementary Information (ESI) available: CCDC 2325953-2325956. For ESI and crystallographic data in CIF or other electronic format see DOI: 10.1039/x0xx00000x.

cooperative C–H activation enables the catalytic dimerization of alkynes with *Z*-selectivity.

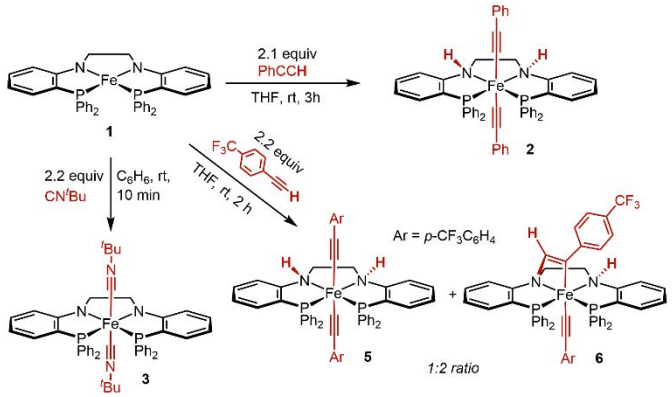

Scheme 1: Reaction of **1** with phenylacetylene, p-trifluoromethylphenylacetylene, and CN^{t}Bu.

Treatment of **1** with 2.1 equiv of phenylacetylene results in the formation of a single new diamagnetic product (**2**, Scheme 1). The ^{1}H NMR spectrum of this compound (Figure S18) features two multiplets at 2.6 and 3.1 ppm corresponding to two pairs of magnetically equivalent protons on the ethylene backbone and a broad resonance at 5.8 ppm that is diagnostic of amine protons. The ^{31}P{^{1}H} NMR spectrum of **2** (Figure S19) shows a single resonance at 76.6 ppm, confirming the magnetic equivalence of the phosphine sidearms. These observations are consistent with activation of the terminal C–H bonds of two equivalents of the phenylacetylene across the two Fe–N_{amide} bonds, producing an Fe bis(phenylacetylide) complex.

To confirm the proposed identity of **2**, crystals suitable for single crystal X-ray diffraction studies were grown by the diffusion of methyl *tert*-butyl ether (MTBE) vapor into a concentrated solution of **2** in fluorobenzene at –35 °C. The resulting solid-state structure confirmed the proposed identity of the Fe bis(phenylacetylide) complex (Fig. 2a). Two $[PhC{\equiv}C]^-$ moieties occupy the axial coordination sites of the octahedral Fe center, and the amine-bound H atoms were located in the Fourier difference map. The conversion of the amides to amines is further supported by the significantly elongated Fe–N distances (2.0563(12) Å vs. 1.872(3) Å in **1**),[25] owing both to the weaker basicity of amines relative to amides and the absence of π-donation. The $\nu_{C\equiv C}$ stretching frequency of 2045 cm^{-1} (Figure S21) corresponding to the bound phenylacetylide fragments closely matches other Fe^{II} acetylide complexes reported in the literature.[27] Additionally, the zero-field Mössbauer spectrum (4 K) displays a well-resolved quadrupole doublet with an isomer shift (δ) of 0.214 mm/s and a quadrupole splitting ($|\Delta E_Q|$) of 1.971 mm/s (Fig. 2b). This isomer shift compares favorably to related low-spin (PNNP)-ligated Fe^{II} complexes.[25,26] Despite the activation of two C-H bonds, an overall four-electron process, these data support maintenance of the Fe^{II} oxidation state via heterolytic cleavage of the alkyne C-H bonds across the Fe-amide bonds.

We next sought to determine if C–H activation is possible for other alkyne substrates and hypothesized that the involvement of the amide would introduce a pK_a dependence. To test this, we attempted reactions of **1** with *tert*-butyl acetylene, trimethylsilyl acetylene, and 1-octyne, all of which are expected to have pK_a values higher than that of phenylacetylene. The ^{1}H NMR spectra for these reactions (Figures S22-S24) demonstrate that no C-H activation was achieved, as the spectra contain only the paramagnetically shifted resonances of **1** and the diamagnetic resonances of the unreacted alkyne. Recognizing the confounding steric effect introduced by switching from phenylacetylene to the tertiary alkylacetylenes, we attempted the reaction of **1** with *tert*-butylisocyanide (CN^{t}Bu) to determine whether donors with ^{t}Bu groups can bind in both open coordination sites. Addition of 2 equiv CN^{t}Bu to a stirring deep red-brown solution of **1** in C_6H_6 immediately yielded a bright orange solution whose ^{1}H, ^{31}P{^{1}H}, and ^{13}C{^{1}H} NMR spectra (Figures S25-S27) are consistent with a symmetric diamagnetic complex (**3**, Scheme 1). Indeed, X-ray diffraction analysis of single crystals of **3** (Figure S14) confirmed that both equivalents of CN^{t}Bu had bound to the open axial Fe coordination sites of **1**. Therefore, we can conclude that the absence of reactivity of **1** with TMSCCH and ^{t}BuCCH is not the result of steric hindrance and is attributed to the diminished acidity of the C-H bonds in these substrates.

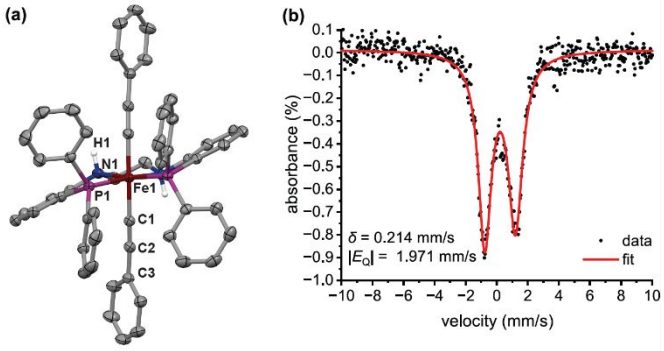

Fig. 2: (a) Displacement ellipsoid (50%) representation of **2**. For clarity, carbon-bonded H atoms and fluorobenzene solvent molecules are omitted, and symmetry-equivalent positions of the asymmetric unit are shown to provide a complete molecular representation. Relevant interatomic distances (Å) and angles (°): Fe1–P1: 2.1750(4), Fe1–N1: 2.0563(12), Fe1–C1: 1.9322(15), C1–C2: 1.219(2), C1–Fe1–C1′: 171.38(9), Fe1–C1–C2: 171.45(13), C1–C2-C3: 175.97(16). (b) Fitted zero-field ^{57}Fe Mössbauer spectrum of **2** at 4 K.

Encouraged by the terminal C–H activation observed stoichiometrically, we next sought to determine whether **1** could effect catalytic dimerization of terminal alkynes. Noting the lack of activation of aliphatic alkynes, we focused our attention predominantly on *para*-substituted phenylacetylene derivatives (Table 1). Phenylacetylene (**4a**) was, indeed, dimerized in >98% conversion in 2 h at 30 °C using 1 mol % loading of **1** in C_6D_6, with an isolated yield of 95% and a *Z:E* ratio of 96:4. The substrate scope was expanded to include both electron-donating and electron-withdrawing groups in the *para* position (Table 1). Substitution with an electron-donating *tert*-butyl substituent at the *para* position in **4b** resulted in a decrease in both conversion/yield (54%/53%) and *Z*-selectivity (*Z*:*E* ratio: 70:30). The addition of electron-withdrawing F (**4c**), Br (**4d**), and CF_3 (**4e**) *para* substituents resulted in decreased isolated yields relative to **4a**; however, excellent *Z*-selectivity was maintained. Finally, the aniline functional group in **4f** inhibited catalytic turnover almost entirely. To rule out the possibility that precursors to **1** could be performing the catalysis, we attempted reactions of $FeCl_2$ and the PN^HN^HP

ligand with PhCCH, and no conversion to product was noted in either case, as confirmed by GC-MS analysis of the crude reaction mixtures (Figures S38 and S39).

Table 1: *Z*-selective catalytic dimerization of alkynes catalyzed by **1** including conversions of alkyne and enyne dimer yields (in parentheses), both determined using ^{1}H NMR spectroscopy.

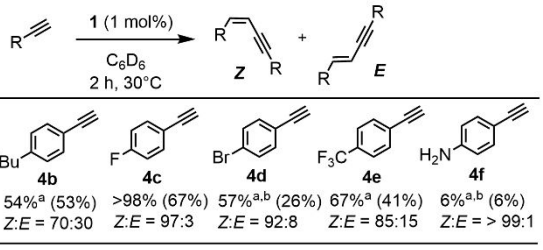

4a	4b	4c	4d	4e	4f
>98% (95%)	54%[a] (53%)	>98% (67%)	57%[a,b] (26%)	67%[a] (41%)	6%[a,b] (6%)
Z:*E* = 96:4	*Z*:*E* = 70:30	*Z*:*E* = 97:3	*Z*:*E* = 92:8	*Z*:*E* = 85:15	*Z*:*E* = > 99:1

[a] No further conversion was noted upon stirring for 24 h.
[b] Due to lack of conversion with 1 mol %, 5 mol % **1** was used.

Analysis of the **1**/**4a** reaction mixture post-catalysis by ^{31}P{^{1}H} NMR spectroscopy (Figure S2) revealed **2** with a small amount of an unsymmetric Fe-containing species (vide infra) and a small amount of ligand-based decomposition. To probe whether **2** is a catalytically active species, the isolated complex was evaluated as a catalyst under identical reaction conditions (1 mol %, 30 °C, 1 h), resulting in conversion to 1,4-diphenylbut-1-en-3-yne as confirmed by GC-MS and ^{1}H NMR spectroscopic analyses (Figures S36 and S37). This result indicates that **2** is, itself, catalytically active and that it, or a singly activated PhCCH analogue, is likely an intermediate along the dimerization pathway. The selectivity is slightly diminished when using **2** (86:14 vs 96:4 for **1**), hinting that **2** may be an off-cycle species rather than a direct intermediate (vide infra).

Prompted by the diminished conversion observed for **4e**, which contains a relatively unreactive CF_3 functional group, we investigated the **1**/**4c** and **1**/**4e** catalytic reactions *in situ* using ^{31}P{^{1}H} NMR spectroscopy to determine whether C-H activated bis(acetylide) species analogous to **2** were formed with different phenylacetylene derivatives under the catalytic reaction conditions. Although an analogue of **2** was formed upon treatment of **1** with excess **4c**, in the case of **4e**, an appreciable quantity of a second asymmetric metal complex was observed (Figure S2). Further investigation of the reaction between **1** and **4e** revealed an inseparable 1:2 mixture of a symmetric bis(acetylide) species, **5**, and an unsymmetric species resulting from [2+2] cycloaddition of the alkyne across the Fe-N_{amide} bond, **6** (Scheme 1, see ESI for more details). The formation of this side product may contribute to the diminished yield of enyne from **4e**.

As an initial mechanistic probe, we attempted a crossover experiment between PhCCH and ^{t}BuCCH. We hypothesized that ^{t}BuCCH could only be incorporated into an enyne product if C-H activation of aliphatic alkynes did occur, but reversibly and with a very small and undetectable concentration of C-H activated product formed at any given time. To probe this hypothesis, a catalytic reaction was performed using a vast excess of ^{t}BuCCH (57 equiv) with respect to PhCCH, resulting in the formation of a very small amount of cross-dimerization products (~7%) (Scheme 2a, Figure S40). Although phenylacetylene homodimerization products comprised the majority of the product mixture (93%), the formation of cross-dimerization products is indicative of reversible activation of the C-H bonds of aliphatic alkynes. Although a coordination-insertion mechanism could also explain the formation of the cross-dimerization products, the lack of detection of the *gem* enyne isomer under any conditions suggests that a coordination-insertion mechanism is not operative. A subtle interplay between the steric and electronic factors governing 1,2-insertion and 2,1-insertion of alkyne into an Fe–acetylide bond to form the *gem* and *Z* isomers would be expected if such a mechanism was at play.

Scheme 2. Experiments performed to probe the mechanism of alkyne dimerization by **1**.

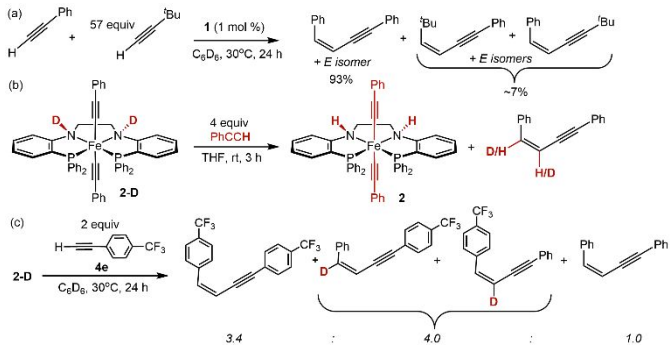

We next sought to further elucidate the alkyne dimerization mechanism with deuterium-labelling experiments. Treatment of **1** with PhCCD produces a diamagnetic species **2-D** whose ^{1}H NMR spectrum is consistent with **2** but lacks the peak corresponding the N–H protons (Figure S41). Upon treatment of **2-D** with 4 equiv of PhCCH, the broad ^{1}H NMR resonance at 5.81 reappears in the NMR spectrum (Figure S42) and turnover to the phenylacetylene dimer is observed, with ^{2}H incorporation into the organic dimer detected by ^{2}H NMR spectroscopy (Scheme 2b, Figure S43). This result confirms that proton transfer between the alkyne and amides is reversible and part of the mechanism of alkyne dimerization by **1**. Additionally, if isolated **2-D** is treated with 2 equiv of **4e**, both possible homodimers and the cross-dimerization product are detected (Scheme 2c, Figure S44). The detection of the cross dimer suggests that **2-D** is in equilibrium with a singly activated acetylide complex, as cross-dimer formation would require exchange with one of the bound phenylacetylide ligands in **2-D**. Consistent with this hypothesis, GC-MS analysis indicated that the two of **4a**/**4e** cross-dimerization products, which could not be separated by GC, were predominantly singly deuterated (Figure S44). Interestingly, the ratio of products observed in the cross-dimerization experiment deviates substantially from a statistical 1:2:1 distribution, with a 3.4:4:1 ratio between the homodimer of **4e**, the **4a**/**4e** cross-dimer, and the homodimer of **4a**. The preference for dimerization of **4e** may be explained by its greater acidity, allowing for more facile C–H bond activation.

Due to the redox neutrality of the alkyne dimerization processes in general, the possible non-radical mechanisms are largely invariant of metal identity and include two main possibilities: (1) coordination-insertion, and (2) nucleophilic attack of the electrophilic α-carbon of a vinylidene by a bound

metal-acetylide.[10–13,18,19,22] This, coupled with the experiments described previously, leads us to propose a catalytic cycle in which **1** activates an alkyne C–H bond across one Fe–N_{amide} bond to form a mono(acetylide) complex **A** (Fig. 3). We posit that **A** exists in equilibrium with **2** through reversible activation of a second equiv of alkyne, but that **2** is an off-cycle intermediate. From **A**, an intramolecular proton transfer could form monovinylidene compound **B**. A second equiv of alkyne could then attack the vinylidene α-carbon and protonate the amide to form the alkynyl vinyl intermediate **C**, through either a concerted or stepwise process. A final proton transfer could liberate the final organic product and regenerate **1**. The stereochemistry of the alkene would be set upon formation of **C**, and the proposed mechanism is consistent with the observed *Z* preference, as this minimizes steric clash between the alkene substituent and the (PNNP) phenyl groups.

Interestingly, other accepted mechanisms for Fe-catalyzed *Z*-selective dimerization in the literature—including those of Kircher and Milstein—do not invoke metal-ligand cooperativity, as D-labelling experiments in both cases showed that D was not incorporated into the ligand. Our proposed mechanism invokes metal-ligand cooperativity in two different steps, distinguishing this work from the present literature.

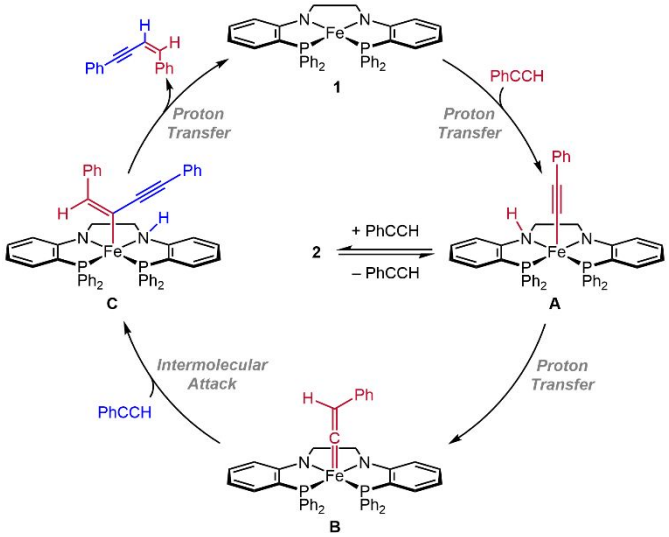

Fig. 3: Proposed catalytic cycle of alkyne dimerization by **1**.

In conclusion, we have shown that **1** can activate the terminal C–H bonds of aryl alkynes across its Fe–N_{amide} bonds to produce an Fe bis(acetylide) complex **2**. Complex **1** was also shown to catalyze the *Z*-selective dimerization of aryl alkynes in moderate to excellent yields under mild conditions. Based on a series of stoichiometric experiments, we propose a unique metal-ligand cooperative catalytic cycle that proceeds through a vinylidene intermediate, distinguishing this result from existing literature.[21–23]

This study was supported by the U.S. National Science Foundation under Grant CHE-2101002.

Conflicts of interest

There are no conflicts to declare.

Notes and References

1 P. Wessig and G. Müller, *Chem. Rev.*, 2008, **108**, 2051–2063.
2 I. H. Goldberg, *Acc. Chem. Res.*, 2002, **24**, 191–198.
3 M. Barday, K. Y. T. Ho, C. T. Halsall and C. Aïssa, *Org. Lett.*, 2016, **18**, 1756–1759.
4 X. Zhou, C. Huang, Y. Zeng, J. Xiong, Y. Xiao and J. Zhang, *Chem. Commun.*, 2017, **53**, 1084–1087.
5 V. V. Pagar and T. V RajanBabu, *Science*, 2018, **361**, 68–72.
6 B. Kang, D. Kim, Y. Do and S. Chang, *Org. Lett.*, 2003, **5**, 3041–3043.
7 R. Chinchilla and C. Nájera, *Chem. Rev.*, 2007, **107**, 874–922.
8 E. Negishi and L. Anastasia, *Chem. Rev.*, 2003, **103**, 1979–2018.
9 B. M. Trost and J. T. Masters, *Chem. Soc. Rev.*, 2016, **45**, 2212–2238.
10 R. Hua, in *Addition Reactions with Unsaturated Hydrocarbons*, ed. R. Hua, Wiley, 2022, pp. 1–31.
11 S. Weon Roh, K. Choi and C. Lee, *Chem. Rev.*, 2019, **119**, 4293–4356.
12 Q. Liang, K. Hayashi and D. Song, *ACS Catal.*, 2020, **10**, 4895–4905.
13 S. M. Weber and G. Hilt, *Front. Chem.*, , DOI:10.3389/fchem.2021.635826.
14 G. C. Midya, B. Parasar, K. Dhara and J. Dash, *Org. Biomol. Chem.*, 2014, **12**, 1812–1822.
15 G. C. Midya, S. Paladhi, K. Dhara and J. Dash, *Chem. Commun.*, 2011, **47**, 6698–6700.
16 M. Bhunia, S. R. Sahoo, G. Vijaykumar, D. Adhikari and S. K. Mandal, *Organometallics*, 2016, **35**, 3775–3780.
17 F. Xue, X. Song, T. T. Lin, K. Munkerup, S. F. Albawardi, K.-W. Huang, T. S. A. Hor and J. Zhao, *ACS Omega*, 2018, **3**, 5071–5077.
18 Q. Liang, K. Sheng, A. Salmon, V. Y. Zhou and D. Song, *ACS Catal.*, 2019, **9**, 810–818.
19 Q. Liang, K. M. Osten and D. Song, *Angew. Chem. Int. Ed.*, 2017, **56**, 6317–6320.
20 Q. Liang, K. Hayashi, K. Rabeda, J. L. Jimenez-Santiago and D. Song, *Organometallics*, 2020, **39**, 2320–2326.
21 O. Rivada-Wheelaghan, S. Chakraborty, L. J. W. Shimon, Y. Ben-David and D. Milstein, *Angew. Chem. Int. Ed.*, 2016, **55**, 6942–6945.
22 N. Gorgas, B. Stöger, L. F. Veiros and K. Kirchner, *ACS Catal.*, 2018, **8**, 7973–7982.
23 N. Gorgas, L. G. Alves, B. Stöger, A. M. Martins, L. F. Veiros and K. Kirchner, *J. Am. Chem. Soc.*, 2017, **139**, 8130–8133.
24 S. Garhwal, N. Fridman and G. de Ruiter, *Inorg. Chem.*, 2020, **59**, 13817–13821.
25 G. P. Hatzis and C. M. Thomas, *Chem. Commun.*, 2020, **56**, 8611–8614.
26 J. E. Stevens, C. E. Moore and C. M. Thomas, *J. Am. Chem. Soc.*, 2023, **145**, 794–799.
27 C. Vance Thompson, A. L. Narro, H. D. Arman and Z. J. Tonzetich, *Organometallics*, 2022, **41**, 2291–2300.